JMEPEG (2004) 13:64-68
DOI: 10.1361/10599490417515

1059-9495/$19.00

The Influence of Nickel and Copper on the Austempering of Ductile Iron

U. Batra, S. Ray, and S.R. Prabhakar

(Submitted 2 July 2003; in revised form 6 November 2003)

In the present investigation, the effect of alloying elements on the austempering process, austempered microstructure, and structural parameters of two austempered ductile irons (ADI) containing 0.6% Cu and 0.6% Cu /1.0% Ni as the main alloying elements was investigated. The optical metallography and x-ray diffraction were used to study the changes in the austempered structure. The effect of alloying additions on the austempering kinetics was studied using the Avrami equation. Significantly more upper bainite was observed in the austempered Cu-Ni alloyed ADI than in Cu alloyed ADI. The volume fraction of retained austenite (X_γ), the carbon level in the retained austenite (C_γ), and the product $X_\gamma C_\gamma$ in an austempered structure of Cu-alloyed ADI are higher than in Cu-Ni-alloyed ADI. The austempering Kinetics is slowed down by the addition of Ni.

Keywords alloying addition, austempering, austenitization, bainitic transformation, retained austenite

1. Introduction

The base iron chemistry and alloy additions in ductile iron play important roles in austempered ductile iron (ADI) technology. The addition of alloying elements to ductile irons, for the production of ADI are often considerably higher than the levels used for the production of conventional grades of ductile iron.[1] The majority of ADI components need to be alloyed for satisfactory austemperability. Alloying element additions serve to delay the transformation of austenite in ductile iron.[2-4] The importance of alloying additions depends upon their relative effectiveness on the reactions in stage I and stage II of the austempering process. The effect of silicon and the individual or combined additions of copper (Cu), molybdenum (Mo), nickel (Ni), and manganese (Mn) on the transformation characteristics of ADI have been reported earlier.[2,5–7] Mn and Mo delay the reactions in stage I and stage II of the austempering process. Cu does not effect the carbon diffusion in austenite or the stability of austenite. However, it has been reported that Cu suppresses carbide formation in lower bainite.[8] Ni acts in a similar way to Cu. If Ni is present in excess of 0.5%, it slows down the bainitic reaction, and thus, causes the formation of martensite at austenite cell boundaries on cooling. The findings on the influence of additions of Ni and Cu on austempering are reported and discussed in this paper. The effect of austenitization and austempering parameters on the austempering process has already been reported for the Cu alloyed ductile iron used for the current study.[9,10]

U. Batra, Department Of Metallurgical Engineering, Punjab Engineering College, Chandigarh, India; **S. Ray,** Department of Metallurgical and Materials Engineering, IIT Roorkee, India; and **S.R. Prabhakar,** Principal, Indo Global College of Engineering and Technology, India. Contact e-mail: umabatra2@yahoo.com.

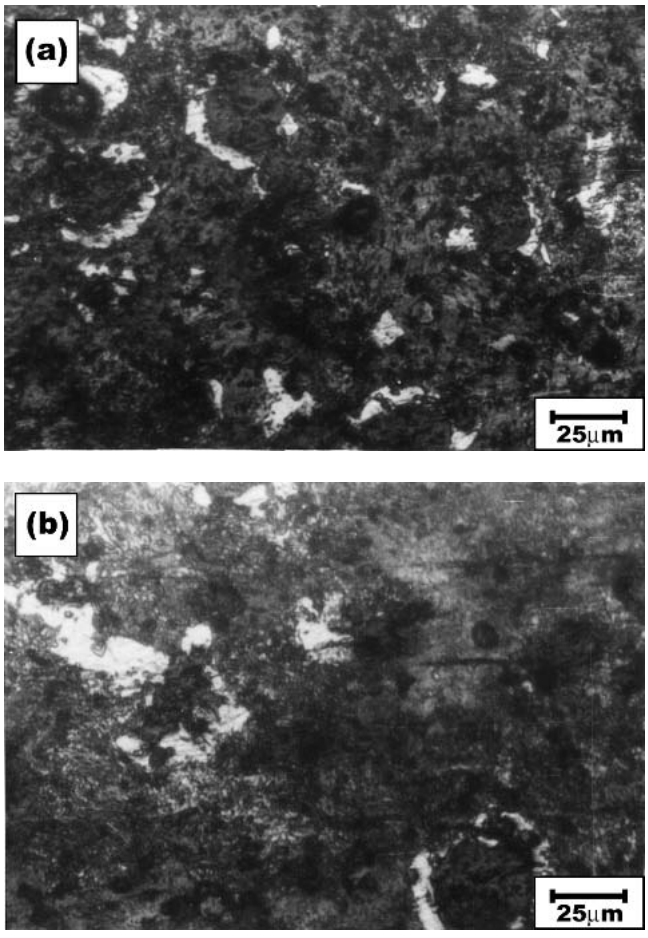

Fig. 1 Microstructure of cast ductile irons **(a)** copper alloyed iron and **(b)** copper-nickel alloyed iron

2. Experimental Procedure

Two ductile irons (Fe) with chemical compositions: (a) 3.48C, 2.028Si, 0.22Mn, 0.05Cr, 0.016Ni, 0.6Cu, 0.04Ti,

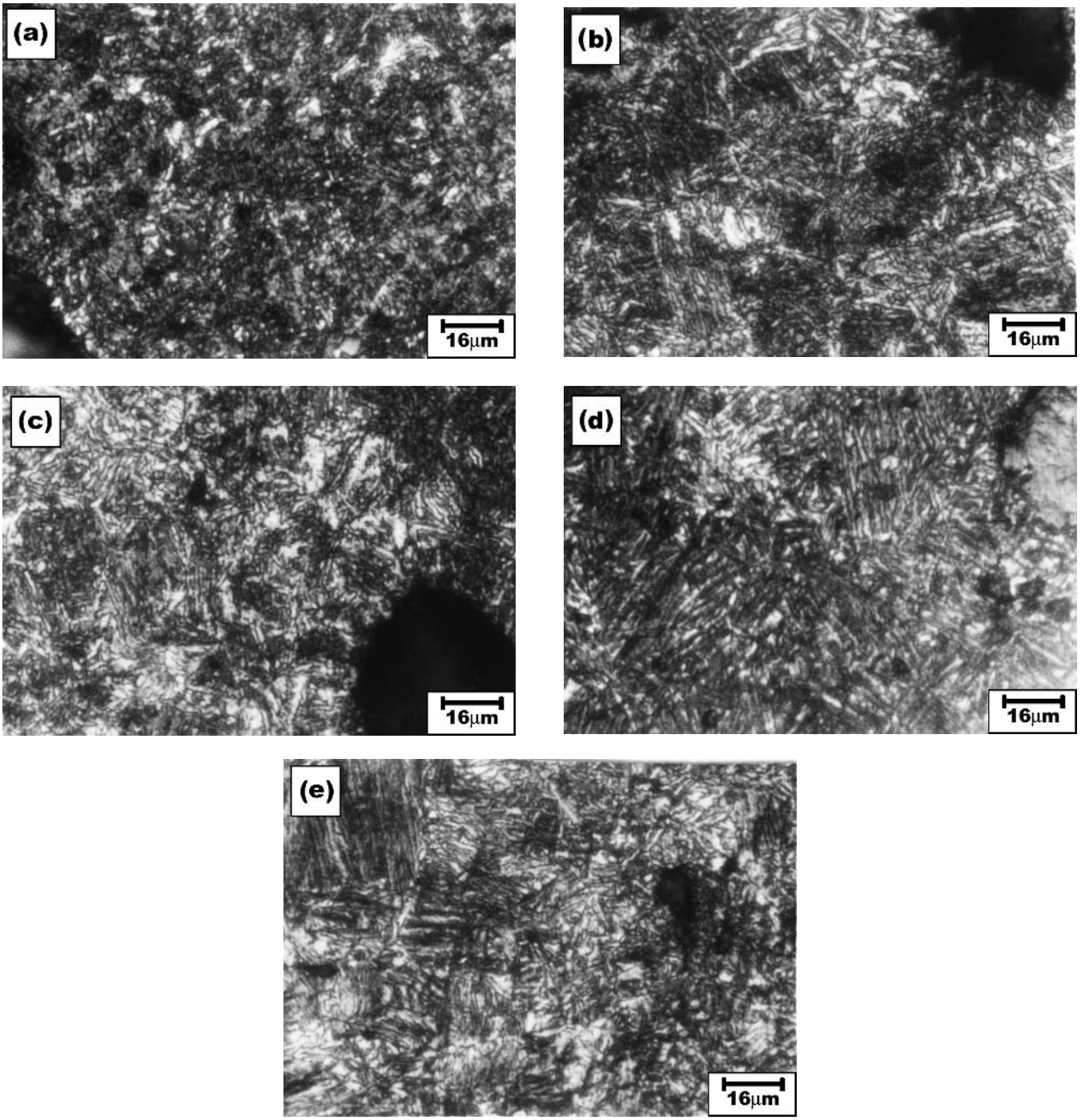

Fig. 2 Microstructure of Cu alloyed ADI after austenitization at T_γ = 850 °C for t_γ = 120 min and austempering at a fixed temperature of 330 °C for various times, t_A: **(a)** t_A = 30 min, **(b)** t_A = 60 min, **(c)** t_A = 90 min, **(d)** t_A = 120 min, **(e)** t_A = 150 min

Table 1 Microstructural Characteristics of Cast Irons

Characteristics	Cu–Iron	Ni–Cu Iron
Nodule size, mm	0.04	0.043
Nodule count	250	198
Amount of ferrite, %	5	4
Amount of pearlite, %	95	96

0.03Mo, 0.0079Sn, 0.012V, 0.02Al, balance Fe, and (b) 3.48C, 1.83Si, 0.23Mn, 0.01Cr, 1.05Ni, 0.6Cu, 0.04Ti, 0.015Mo, 0.0046Sn, 0.002V, 0.02Al, balance Fe, were prepared in a commercial foundry using an induction melting furnace and cast in the shape of 25 mm (1 in) Y blocks. The cast microstructures of Cu alloyed and Cu-Ni alloyed ductile irons under study are shown in Fig. 1. Their microstructural characteristics are given in Table 1. Un-notched Charpy specimens of size 55 × 10 × 10 mm as per ASTM specifications A327-80 were

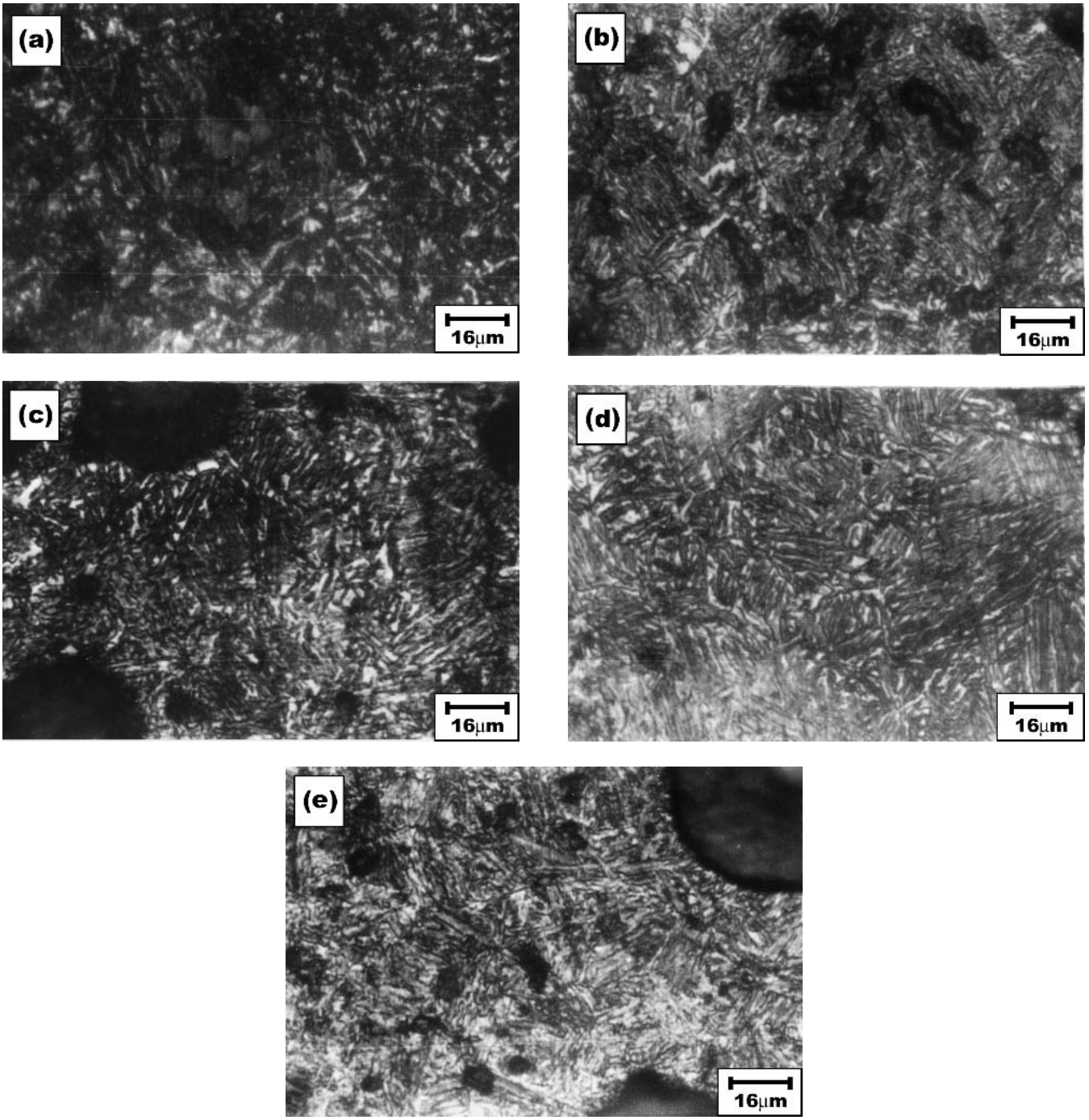

Fig. 3 Microstructure of Cu-Ni alloyed ADI after austenitization at T_γ = 850 °C for t_γ = 120 min and austempering at a fixed temperature of 330 °C for various times, t_A: **(a)** t_A = 30 min, **(b)** t_A = 60 min, **(c)** t_A = 90 min, **(d)** t_A = 120 min, **(e)** t_A = 150 min

machined from the leg part of the Y block castings of both ductile irons.[11] The samples were austenitized at 850 °C for 120 min and transferred rapidly to a salt bath held at 330 °C for austempering for different time periods before quenching in water. Samples for metallography were polished, etched, and examined using standard metallographic techniques. The average volume fraction of austenite, X_γ and its average carbon content, C_γ in the austempered structure were determined using x-ray diffraction patterns taken with Cu K_α radiation (λ = 1.54 Å).[12] The mean size of the bainitic ferrite particles d_α was calculated from these patterns using the Scherer equation.[12]

3. Results and Discussion

The microstructure of cast Cu alloyed and Cu-Ni alloyed ductile Fe contains graphite nodules in a ferrite-pearlite ma-

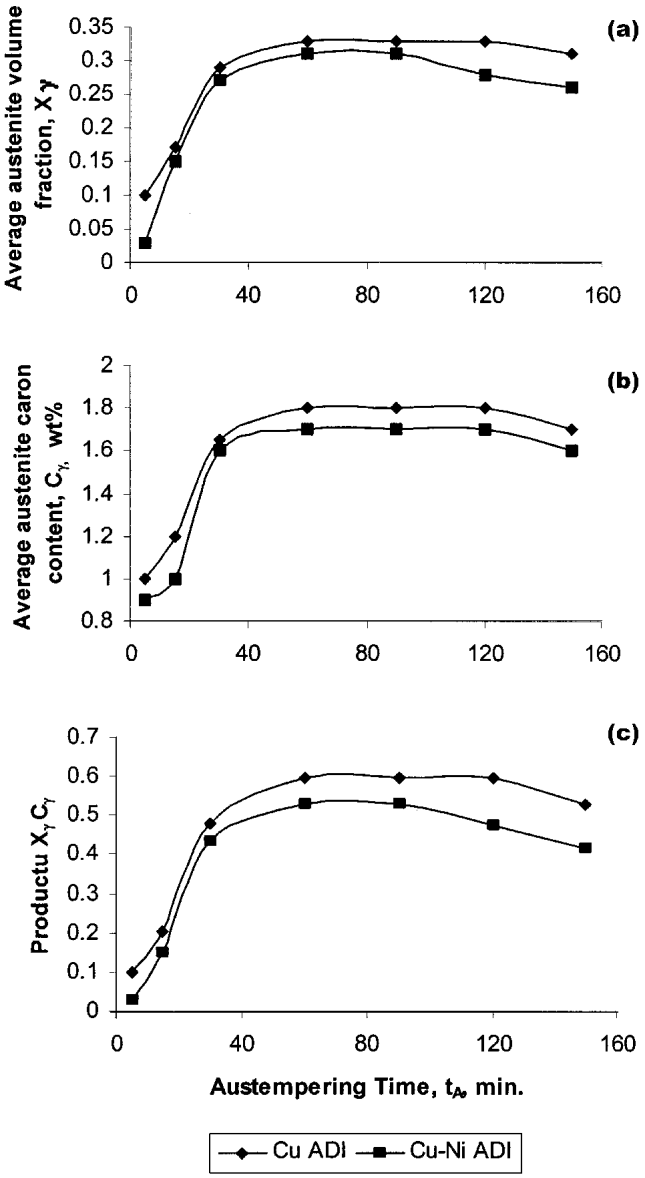

Fig. 4 Variation of **(a)** volume fraction of retained austenite, X_γ **(b)** average austenite carbon content, C_γ, and **(c)** product $X_\gamma C_\gamma$ in austempered Cu alloyed ADI and Cu-Ni alloyed ADI with austempering time at 330 °°C after austenitization at T_γ = 850 °C for 120 min

trix as can be observed in Fig. 1(a) and 1(b), respectively. The effect of austempering time and alloy composition has been studied on the austempered microstructure, structural parameters, and austempering kinetics for both the ductile Fe when the samples were austenitized at 850 °C for 120 min and subsequently austempered at 330 °C for different time periods. The austempered microstructures of Cu alloyed ADI are given in Fig. 2(a-e) when the Fe is austempered at 330 °C for 30, 60, 90, 120, and 150 min, respectively, after austenitization at 850 °C for 120 min. The ADI, austempered for 30 min consists of a substantial amount of martensite and small amounts of bainitic ferrite and retained austenite. At the longer austempering time of 60 min, the structure consists of bainitic ferrite and retained austenite, and no martensite is visible in the micro-

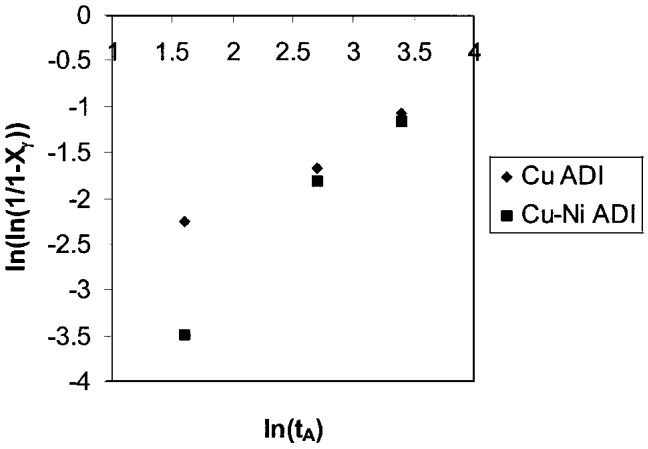

Fig. 5 Variation of $\ln[\ln(1/1\text{-}X_\gamma)]$ with $\ln(t_A)$ during growth part of austempering process for a fixed austempering temperature of T_A = 330 °C in Cu alloyed ADI and Cu-Ni alloyed ADI.(T_γ = 850 °C, t_γ = 120 min)

structure. Further increase in the austempering time to 150 min did not result in any noticeable change in the microstructure. During the austempering process, the bainitic ferrite forms by rejection of carbon (C) into the residual austenite. As the austempering progresses, more of bainitic transformation occurs accompanied by rejection of more C into the surrounding austenite resulting in the increase in the amount of austenite and the amount of C in the austenite. In earlier stages, the C content of austenite is insufficient to make it stable, and therefore, it transforms to martensite. However, at longer times, C enrichment of austenite may be sufficient to result into retained austenite on cooling.

The austempered microstructures of the Cu-Ni alloyed ADI are given in Fig. 3(a-e). At a short austempering time of 30 min, the austempered microstructure consists of martensite only. At a longer austempering time of 60 min, there is an appreciable decrease in the amount of martensite and an increase in the amounts of bainitic ferrite and retained austenite. At a still longer austempering time of 90 min, the microstructure consists of bainitic ferrite and retained austenite with no martensite observed. There is no noticeable change in the microstructure with a further increase in austempering time to 150 min.

On comparing the austempered microstructure of Cu-alloyed ADI, one could observe a relatively higher amount of upper bainite in Cu-Ni alloyed ADI than that in Cu alloyed ADI. Also the upper bainite is coarser. This implies that the addition of Ni lowered the bainitic transformation temperature range resulting in transformation to upper bainite.

The volume fraction of retained austenite, X_γ, its Cu content, C_γ, and the product of $X_\gamma C_\gamma$ in the austempered structure are compared in Fig. 4 for the ADI austenitized at 850 °C for 120 min and subsequently austempered at 330 °C for different austempering time periods of between 30-150 min. One may observe that the trend in variation of X_γ, C_γ, and $X_\gamma C_\gamma$ with austempering time is similar in Cu-alloyed and Cu-Ni-alloyed ADI. The formation of upper bainite in Cu-Ni ADI during austempering rejects an increased level of C to the surrounding austenite.

Table 2 Austempering Transformation Kinetics Parameters

Sample	Austenization Temperature, (T_γ) °C	Austenization Time, (t_A) min	Austempering Temperature, (T_A) °C	m	K
Cu–alloyed ADI	850	120	330	0.64	0.036
Ni–Cu–alloyed ADI	850	120	330	0.86	0.020

The kinetics of the austempering process has been studied using Avrami equations of the type[13]:

$$X_\gamma(t) = 1 - \exp(-kt^m) \quad \text{(Eq 1)}$$

where $X_\gamma(t)$ is the volume fraction of the retained austenite formed after an austempering time t, and k and m are constants for the reaction and can be determined experimentally. If k and m are known, the kinetics of the reactions may be predicted for a given set of conditions. Rearranging Eq 1 and taking the log twice,

$$\ln[\ln(1/1 - X_\gamma)] = m \ln(t_A) + \ln(k) \quad \text{(Eq 2)}$$

A plot of $\ln[\ln(1/1\text{-}X_\gamma)]$ against $\ln(t_A)$ would be a straight line with a slope m and intercept, ln (k). These plots have been drawn for Cu-alloyed and Cu-Ni-alloyed iron for the austenitization and austempering conditions considered in the current study and are shown in Fig. 5. From Fig. 4 it may be observed that there is a considerable incubation period for austempering transformations and the product austenite is not stable throughout the austempering process. At short austempering times, X_γ is small, but it increases with further increase in the austempering time, reaching a plateau value and then decreasing at long austempering times. These factors are not accounted for in the general Avrami equation which assumes short incubation periods compared with the time required for the reaction to complete and the formation of stable reaction products. Hence, to accommodate these differences only the growth part of the process is considered in determining m and k. The values of m and k thus obtained from Fig. 5 are given in Table 2. These results confirm that the presence of Ni in the base iron decreases the reaction rate of stage I austempering.

4. Conclusions

ADI alloyed with Cu-Ni has higher amounts of upper bainite than ADI alloyed with Cu when austenitized and austempered under the similar conditions. The addition of Ni shifts the bainitic transformation temperature down corresponding to higher transformation products in Cu-Ni-alloyed ADI. The presence of Ni in base ductile iron decreases the reaction rate of stage I austempering.

References

1. B.V.S.K. Sastry: "Studies on Some Characteristics of ADI," Ph.D. Thesis, IIT Kharagpur, India, 1993, pp. 70-80.
2. E. Dorazil, B. Barta, E. Munsterova, L. Stransky, and A. Huvar: "High-Strength Bainitic Ductile Cast Iron," *AFS Int., Cast Metals J.*, 1982, *2*(7), pp. 52-62.
3. M. Johansson: "Properties and Application of Austempered Austenitic-Bainitic Ductile Iron," *Trans AFS*, 1977, *85,* pp. 117-22.
4. T.N. Rouns, D.J. Moore, and K.B. Rundman: "On the Structure and Mechanical Properties of Austempered Ductile Iron," *Trans. AFS*, 1984, *92,* pp. 815-40.
5. J. Dodd: "High Strength, High Ductility, Ductile Irons," *Modern Casting*, 1978, *68,* pp. 60-66.
6. K.B. Rundman and T.N. Rouns: "On the Effects of Molybdenum on the Kinetics of Secondary Graphatization in Quenched and Tempered Ductile Irons," *Trans AFS,* 1982, *90,* p. 487.
7. M. Gagne: "Influence of Manganese and Silicon on the Microstructure and Tensile Properties of Austempered Ductile Iron," *Trans AFS,* 1985, *93,* p. 801.
8. R. Elliott: *Cast Iron Technology*, Jaico Publishing House, Bombay, India, 1995.
9. U. Batra, S. Ray, and S.R. Prabhakar: "Austempering and Austempered Ductile Iron Microstructure in Copper Alloyed Ductile Iron," *J. Mater. Eng. Performance,* 2003, *12*(4), pp. 426-29.
10. U. Batra, S. Ray, and S.R. Prabhakar: "Effect of Austenitization on Austempering of Copper Alloyed Ductile Iron," *J. Mater. Eng. Performance,* 2003, *12*(5), pp. 597-601.
11. K.D. Mills: "Spheroidal Graphite Cast Iron—Its Development and Future," *Brit. Foundryman*, 1972, *65,* p. 34.
12. B.D. Cullity: *Elements of X-Ray Diffraction*, Addison Wesley Publishing Company, Inc., Reading, MA, 1956, pp. 390-96.
13. J. Achary: "Thermomechanical Processing of Ductile Iron," Ph.D. Thesis, Univ. of Wisconsin, Milwaukee, WI, 1995, pp. 65-77.